# MECHANICS OF SPERM-EGG INTERACTION AT THE *ZONA PELLUCIDA*

JAY M. BALTZ, DAVID F. KATZ,* AND RICHARD A. CONE
*The Jenkins Department of Biophysics, The Johns Hopkins University, Baltimore, Maryland 21218; and *Departments of Obstetrics and Gynecology, and Chemical Engineering, University of California, Davis, California 95616*

ABSTRACT Mammalian sperm traverse several layers of egg vestments before fertilization can occur. The innermost vestment, the *zona pellucida*, is a glycoprotein shell, which captures and tethers the sperm before they penetrate it. We report here direct measurements of the force required to tether a motile human sperm as well as independent calculations of this force using flagellar beat parameters observed for sperm of several species on their homologous *zonae*. We have compared these sperm-generated forces with the calculated tensile strength of sperm-*zona* bonds, and found that a motile sperm can be tethered, at least temporarily, by a single bond. Therefore, sperm can be captured by the first bond formed and tethered permanently by a few. The sperm cannot subsequently penetrate the *zona* unless the bonds are first eliminated. However, premature elimination would simply allow the sperm to escape. Therefore, not only must the bonds be eliminated, but the timing of this must be regulated so that the sperm is already oriented toward the egg and beginning to penetrate as the bonds are broken.

## INTRODUCTION

The mammalian egg is completely encapsulated by external structures or vestments. The outermost is the cumulus, an hyaluronic acid gel through which the sperm must first penetrate (Talbot, 1985; Talbot et al., 1985). Inside the cumulus is the *zona pellucida*, a glycoprotein shell which is adhesive to sperm but which also forms a final mechanical barrier to sperm penetration. Before reaching the egg plasma membrane, a sperm must first bind to the *zona*, reorient towards the egg, and penetrate the *zona*.

Sperm are captured by their heads upon contacting the *zona* because the sperm head and *zona* surface possess complimentary receptor-ligand pairs (Wassarman, 1987; Lopez et al., 1985; Peterson et al., 1984; O'Rand et al., 1985; Sullivan and Bleau, 1985; Bleil and Wassarman, 1980). The flagellum produces forces on the head which act in directions tending to pull the sperm away from the *zona* during much of each flagellar beat. While the sperm is tethered to the *zona*, the sperm-*zona* bonds must collectively be strong enough to withstand the maximum force with which the flagellum can pull.

Before the sperm can penetrate the *zona*, the flagellum must be able to move the head into the *zona* material which had previously tethered and immobilized it. Therefore, some or all of the adhesion must be eliminated, and it must be done in such a way that the sperm does not simply escape. The flagellar motion of a sperm stuck passively to the *zona* is not sufficient, without a precise interplay between the sperm-*zona* adhesion and sperm motility, to cause penetration. Therefore, the mechanical behavior of the sperm and *zona* from initial contact through penetration needs to be examined.

Green and Purves (1984) were the first to calculate the thrust that a sperm could exert on the *zona*. From the magnitude of the thrust, they concluded that the sperm could mechanically (i.e., nonenzymatically) penetrate the *zona* only if it behaved as a liquid, a purely viscous gel, because the sperm would have a negligible effect on the lifetimes they estimated for the constituent bonds of the *zona* material. Subsequently, Green (1987) found that the *zona* appears to behave primarily as an elastic solid, precluding purely mechanical penetration. Work by other investigators has included more detailed calculation of the thrust that a sperm develops during penetration (Katz and deMestre, 1985). However, calculations of the forces developed by a motile sperm have not been verified by direct calculations, nor have the mechanics of capturing and tethering a sperm to the *zona* and the transition from binding to penetration been examined.

To clarify the mechanics of the sperm-*zona* interaction and help reveal the mechanisms that underlie binding and the onset of penetration, we have: (*a*) both directly measured and calculated the minimum force required to tether a motile sperm cell; (*b*) compared this force with the strength of the bonds likely to hold the sperm on the *zona;* and (*c*) determined what these results imply about the spatial distributions of the sperm-*zona* bonds and the

Please address correspondence to Dr. Baltz at Laboratory of Human Reproduction and Reproductive Biology, Harvard Medical School, 45 Shattuck Street, Boston, Massachusetts 02115.

temporal sequences in which they form and are eliminated.

## MATERIALS AND MEHODS

### A Composition of Solutions

A modified Physiological Salt Solution (Cardullo, 1985; Cardullo and Cone, 1986) designated Physiological Salt Solution D (PSSD) was used in the micropipet experiments. It consisted of 140 mM NaCl, 3.5 mM KCl, 0.9 mM $CaCl_2$, 0.9 mM $MgCl_2$, 12 mM $Na_2HPO_4$, and 2.2 mM $NaH_2PO_4$ (J. T. Baker Chemical Co., Phillipsburg, NJ) at pH 7.3, with 0.08 gm/liter Na Penicillin G (Sigma Chemical Co., St. Louis, MO). The media used during sperm-egg interactions have been described in previous publications (Katz et al., 1986; Suarez et al., 1983; Gould et al., 1983; Katz and Yanigimachi, 1981).

### B Cell Collection and Preparation

Human semen for micropipet experiments was collected by masturbation and allowed to liquefy at 37°C. The motile sperm were then separated from the semen by a swim up procedure in which PSSD was layered on top of semen and allowed to stand for 1.5 h at 37°C while motile sperm separated by their own motility into the PSSD layer. The PSSD supernatant then contained a nearly 100% motile population of sperm ($\sim 10^7$ sperm/ml). The supernatant was collected and BSA (Grade IV; Sigma Chemical Co.) was added to it for a final BSA concentration of 3%. This helped prevent adhesion of the sperm to the pipets.

Sperm for sperm-*zona* interaction studies were collected and capacitated as previously described (guinea pig and hamster: Katz and Yanigimachi, 1981; Katz et al., 1986; rabbit: Suarez et al., 1983; human: Gould et al., 1983). Cumulus-free eggs used for sperm-*zona* interaction studies were collected as previously reported (hamster: Katz and Yanigimachi, 1981; Katz et al., 1986; guinea pig: Katz and Yanigimachi, 1981; rabbit: Suarez et al., 1983; immature human oocytes: Gould et al., 1983).

### C Determination of the Force Exerted by a Sperm Using Suction Micropipets

1. *Theory.* The head of a motile mammalian sperm tends to move in three dimensions (Denehy et al., 1975; Phillips, 1972; Rikmenspoel, 1965), and hence when bound to the *zona* it not only pushes on the *zona*, but also pulls away from it. For the sperm to remain bound, the tensile strength ($F_b$) of the sperm-*zona* bonds must be great enough to withstand the maximum pulling force ($F_p$) exerted by the sperm (Fig. 1 *a*). To mimic the mechanics of a motile sperm stuck to the surface of the *zona*, a suction micropipet was employed to exert a suction force ($F_s$) analogous to the adhesive force, $F_b$ (Fig. 1 *b*). Since the magnitude of $F_s$ could be controlled, it provided a means for measuring the minimum strength of the pulling force and, hence, the minimum net strength required to tether the sperm to the *zona*.

The force exerted by a suction pipet on a surface occluding the opening at its tip is

$$F_s = (P_{out} - P_{in})A, \quad (1)$$

where $P_{in}$ is the pressure inside the pipet, $P_{out}$ is the pressure outside of the pipet (i.e., 1 atmosphere), and $A$ is the area of the opening.

If a motile sperm is being held on the pipet tip by suction alone, the suction force exerted by the pipet on the sperm must be greater than the force with which the sperm pulls against the pipet opening. If the suction force is then lowered slowly (compared with the flagellar beat frequency of the sperm), the sperm will first begin to swim free when the suction force drops just below the maximum pulling force exerted by the sperm. Thus, using Eq. (1) together with the measured area of the opening, the pressure at which each sperm is first able to swim free yields the maximum pulling force exerted by that sperm.

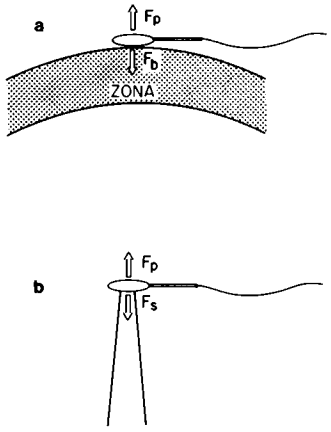


FIGURE 1 The geometry of a sperm on a *zona* and a micropipet. (a) A schematic representation of a sperm adhering to the zona. The sperm pulls on the *zona* with a force $F_p$. The strength of the adhesive force between the sperm and *zona*, $F_b$, must be larger than the pulling force if the sperm is to remain bound. (b) A sperm on a suction micropipet. To mimic the geometry of the sperm on the *zona*, the sperm is held on the pipet with a suction force, $F_s$, which is analogous to the adhesive force between a sperm and *zona*. The orientation of the force vectors shown in this figure are arbitrary. The instantaneous force on the head can act in many directions, as discussed in the text.

2. *Controlling the Suction Force.* The pressure inside the pipet was controled hydrostatically, using the apparatus shown in Fig. 2. The pipet was immersed in the sample chamber (Lucite, with coverslip windows) that contained the sperm sample. If the level in the column was adjusted to be lower than that in the chamber a net pressure pushed into the pipet. The level in the column was precisely controlled by the micrometer-driven syringe. The hydrostatic pressure was

$$P = \rho g \Delta h, \quad (2)$$

where $\rho$ is the density of PSSD with 3% BSA (1.0 g/ml), $g$ is the acceleration due to gravity (980 cm/s$^2$), and $\Delta h$ was the difference in height between the surface level in the chamber and that in the column, obtained from the change in the volume contained in the syringe. The suction force was then found using Eq. (1) with $P = P_{out} - P_{in}$.

To verify that the actual suction force was equal to the calculated suction force, glass beads (Heat Systems-Ultrasonics Inc., Plainview, NY) of known weights (density = 2.66 ± 0.05 gm/cm$^3$; diameters measured by calibrated eyepiece reticle) were picked up with a pipet and the apparent weight of each measured by lowering the pressure until the bead fell off. The measured and true weights of the beads were found to agree satisfactorily (mean difference = 8%, SD = 28%, $n$ = 53).

Unlike the beads, the weight of sperm is undetectably small in this system (<0.01 μdyn). Thus, for sperm, this apparatus detected only motility-related forces. Two other possible sources of error in force determination, compliance of the system and perturbation of the column height by flow into the pipet, were both negligible. Calculation of the flow and measurement of the compliance showed that the error in the force measurements due to each was <0.01%.

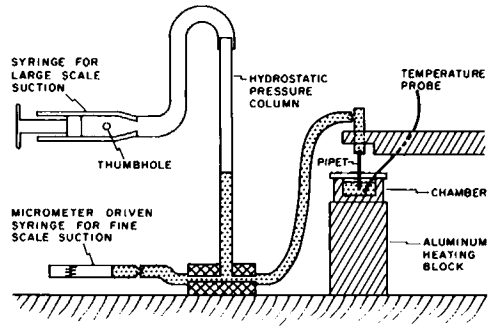


FIGURE 2 The suction micropipet apparatus used to measure the force exerted by a motile sperm. See text for description.

3. *Suction Micropipets.* The glass stock for micropipets was 1.5 mm outer diameter thin wall tubing in 100-mm lengths (Glass Co. of America, Inc. Bargaintown, NJ), used without any treatment. Micropipets were pulled either on a PN-3 horizontal pipet puller (Narishige Lab., Tokyo, Japan), or a 720 vertical pipet puller using the two stage patch pipet option (David Kopf Instruments, Tujunga, CA). The diameters of the pipet openings were measured from photographs. The areas of the openings could be determined in this way to within ±20%. The pipets were treated with a vapor of bis(dimethylamino)dimethylsilane (Fluka Chemical Co., Hauppauge, NY) for 2 min to render them less sticky to the sperm cells.

4. *Procedure for Force Measurement.* Before each force measurement, the suction force was zeroed by adjusting the micrometer driven syringe until one of the very small pieces of debris that invariably appeared in the pipet tip stopped moving, indicating that there was no suction. All force measurements were made relative to this baseline.

For the force measurements, a sperm was first captured using the large scale suction (see Fig. 2) which was then released, so that the sperm was held only by the suction created by the hydrostatic pressure exerted by the column. The sperm was observed while the syringe was slowly turned to lower this suction. At the moment when the sperm pulled free, manipulation of the syringe ceased and its volume reading was recorded, yielding the maximum pulling force exerted by the sperm.

All experiments were done inside a box where the air temperature was maintained at 35°–37°C. The sperm were viewed using a microscope eyepiece, body, and objectives that were mounted in front of the chamber.

Measurements were made only on sperm that satisfied the following criteria: (*a*) No more than 3 h had elapsed after the end of the swim-up (i.e., no more than 5 h post-ejaculation). (*b*) The captured sperm was oriented so that its head was flat on the pipet opening, i.e., the smallest axis of a cross section of the head was parallel to the axis of the pipet. (*c*) The beating was continuous and regular.

In the course of these experiments, on the order of 10,000 sperm were captured on the end of pipets. Of these 10,000, only ~20 sperm could be used for force measurements. The vast majority of the remainder were caught with their tails inside the pipet, and a few were rejected because of the other criteria above.

## D Determination of the Force Exerted by a Sperm Using Hydrodynamic Calculations

To calculate the force with which a motile sperm pulls on a surface on which it is being held, the length of the flagellum, the beat frequency, and the beat shape are needed (see Appendix).

1. *Beat Frequency on Pipets.* The beat frequency and pulling force were measured consecutively for each sperm. The beat frequency was measured using stroboscopic illumination for the microscope (Digistrobe model 1964; Sargeant Welch Co., Skokie, IL) while the sperm was caught on the pipet just before a force measurement. The strobe was lowered from an initially high frequency (>100/s) until the beating flagellum first appeared to freeze. The frequency at which this occurred, read directly from the digital display on the strobe, was taken to be the beat frequency of the sperm.

Unfortunately, this stroboscopic method could not be used for the lowest beat frequencies because at frequencies lower than ~10/s the strobe was resolved by eye as discrete flashes, and the flagellum did not appear to freeze. Therefore, for such sperm with low beat frequencies, VHS video micrography at 30 frames/s was used (see below). The beat frequency was found by viewing the video recording frame by frame during the interval recorded just before the sperm swimming free.

2. *Beat Shape. Measurement of the Major and Minor Axes of the Flagellar Waveform.* The wave was considered to have an elliptical cross section, with both the major and minor axes perpendicular to the long axis of the sperm and the major axis lying parallel to the largest width of the head (Ishijima et al., 1986; Ishijima and Mohri, 1985; Rikmenspoel, 1965; Denehy et al., 1975). To measure these axes, human sperm were prepared as if for a force measurement. A nylon mesh with 88 micron filaments (Small Parts, Inc., Miami, FL) was coated with polylysine by air-drying a 0.1% solution of polylysine (Sigma Chemical Co.) onto it. When incubated with the sperm, the mesh became coated with sperm attached by their heads. The preparation was viewed using videomicrography, with an Olympus BH2 microscope (Opelco, Washington, DC), Nomarski differential interference contrast optics, and a video camera and recorder (RCA Ultracon camera, Panasonic NV-8550 recorder with a framerate of 30/s, and Scotch T120 HG Color Plus video tape cassettes, all from Visual Sound, Broomall, PA). By searching carefully, a few sperm whose flagella were nearly aligned with the optical axis of the microscope could be found. By focusing on the distal tip of the flagellum, which appeared as a small dot that described an elliptical trajectory, the major and minor axes at the distal end of the flagellum were directly measured.

3. *Observation of the Details of Sperm Coming Off Pipets.* To examine in detail the motion of a sperm escaping from a pipet, the same means of pressure control was used as for the force measurements, but the sample was placed on a slide with the pipet entering from the side for the best viewing. Videomicrography, as described above, was used to record the motion of the sperm. The sample was kept at room temperature (21°C) since cooler sperm beat more slowly and the configuration of the sperm could be recorded many times during each beat.

4. *Beat Parameters for Calculation of the Force Exerted by Sperm on Zonae.* The data on sperm movement on the *zona* derive from previous studies undertaken in the laboratory of one of us (David F. Katz). The majority of these data were previously reported in Katz and Yanigimachi, 1981; Gould et al., 1983; Suarez et al., 1983; and, Katz et al., 1986. These sperm-*zona* interactions occurred at 37°C in vitro in chambers sufficiently deep that the flagellar movement was not encumbered. Flagellar movements were observed using either phase-contrast or Nomarski differential interference contrast optics, and were recorded using high speed cinemicrography (100 frames/s: hamster and guinea pig, Katz and Yanigimachi, 1981) or high speed videomicrography (60 frames/s: hamster, Katz et al., 1986; rabbit, Katz and Overstreet, unpublished, and Suarez et al., 1983; human, Gould et al., 1983). The original studies only summarized the data on sperm movement characteristics. For the purposes of the present work, many of the original cine films and video tapes were reanalyzed frame by frame to obtain more detailed data on the flagellar beat shapes.

# RESULTS

## The Force Exerted by Sperm

We used two independent methods to determine the force with which a sperm can pull on a surface to which it is tethered. In the first, the forces exerted by sperm were measured directly using suction micropipets. In the second, the forces were calculated from flagellar beat parameters that were measured experimentally. The first method was used only for human sperm, as attempts to make these pipet measurements on the sperm of other species were unsuccessful; very few nonhuman sperm were captured on pipet tips in the correct geometry, and these did not seal the pipet opening. The calculations not only corroborated the measurements made on human sperm on pipets, but allowed determination of the forces exerted by the sperm of

other species and sperm on *zonae*. In this way, the forces exerted by the capacitated sperm of several species (guinea pig, hamster, human, and rabbit) bound on their homologous *zonae* were determined.

A *Determination of the Force Exerted by a Human Sperm Using Suction Micropipets.* Fig. 3 shows the maximum pulling force of human sperm from five different samples with five different pipets whose openings had diameters of from 1.0 to 1.5 $\mu$m. For motile sperm (at 35°–37°C), the maximum pulling forces were found to range between 11 and 28 $\mu$dyn, with a mean of 20 ± 1.5 $\mu$dyn (mean ± SEM, $n$ = 15 sperm).

As a control for any residual forces between the sperm and the pipet, the suction force at which immotile human sperm came off each pipet was measured. Immotile sperm should, of course, exert no pulling force other than their negligibly small buoyant force. The suction force at which they came off the pipet should therefore be zero. With silanized pipets and BSA present in the solution, immotile sperm came off at a suction force not much different than the baseline (mean = 0.9 $\mu$dyn ± 0.3 SEM, $n$ = 7), as shown in Fig. 3.

Hydrodynamic theory indicates that the measured pulling force should be linearly proportional to the flagellar beat frequency (see Lighthill, 1975 for review; also Dresdner et al., 1980, and the Appendix). The experimental relationship between measured pulling force and frequency is shown for human sperm in Fig. 4. It exhibits good linearity; the best fit line (by least squares) is given by:

$$F_p(\mu\text{dyn}) = 0.9 f(\text{s}^{-1}) \quad (3)$$

($r$ = 0.959, $N$ = 29, standard error of the estimate = 2.3 $\mu$dyn). Note that the best fit line extrapolates through the origin to within the resolution of the instrument (~1 $\mu$dyn), providing an additional control demonstrating that no significant forces acted on each sperm other than the suction force and the forces produced by the motion of its flagellum. It also indicates that motile sperm were like immotile sperm in that they did not adhere to the pipets.

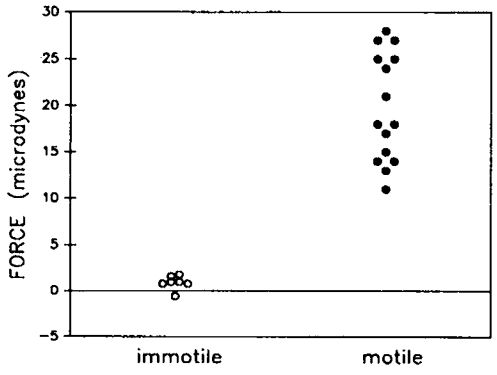


FIGURE 3 The force exerted by human sperm. Each point represents the force measured for a single sperm with the suction micropipet apparatus. Motile sperm: mean force = 20 $\mu$dyn, SEM = 1.5 $\mu$dyn, $n$ = 15. Immotile sperm: mean force = 0.9 $\mu$dyn, SEM = 0.3. $n$ = 7.

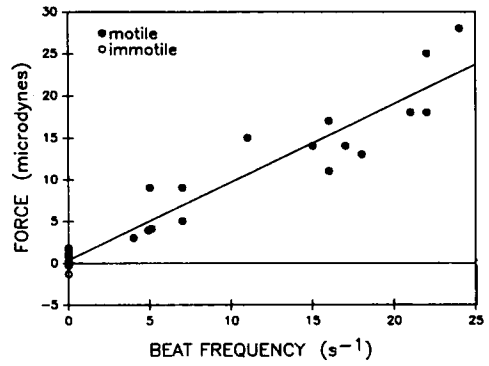


FIGURE 4 The force exerted by human sperm vs. their beat frequency. The forces and beat frequencies were measured for each sperm (each point corresponds to one sperm). The best fit line (by the least squares method) has a slope of 0.9 with a $y$-intercept of 0.4 $\mu$dyn. ($n$ = 29: 16 motile, 13 immotile). Motile sperm with beat frequencies <10/s are from samples that are aged to obtain lower beat frequencies.

B *Determination of the Force Exerted by a Sperm Using Hydrodynamic Calculations*

— 1. METHOD OF CALCULATION. Hydrodynamic theories have been developed that provide the means to calculate the forces produced by a beating flagellum. Our calculations were done using Resistive Force Theory (Gray and Hancock, 1955; Lighthill, 1975, 1976), which is the most widely used. The method is treated in detail in the Appendix.

The time-dependent, three-dimensional waveform of a sperm could not be followed in detail, so an idealized wave shape was used for the calculations. The waveform was represented by a helix of elliptical cross section contained in a conical envelope with its point at the junction of the head and the flagellum (Fig. 7 *c*). Beat amplitudes and frequencies were given the values measured experimentally. For comparison, another waveform, an elliptical helix of constant cross section, was also examined. The results obtained with this waveform (not shown) did not differ greatly from those obtained with the conical helix, indicating that the details of the shape of the waveform are relatively unimportant for the conclusions reached here.

The effect of the hydrodynamic interaction between the flagellum and a nearby surface such as the *zona* is to increase the force developed by the flagellum. But, because the length of the flagellum is comparable with or greater than the diameter of the egg for the species considered and, thus, most of it is far from the surface, this effect is small, less than a factor of two, for this geometry (Katz and deMestre, 1985). Therefore, this correction was not used in these calculations.

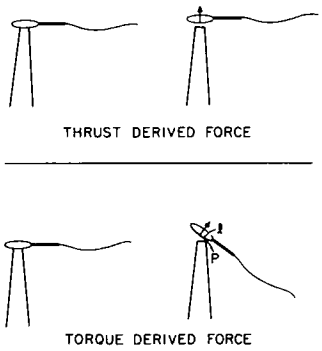


FIGURE 5 Ways that sperm can overcome the suction force of a pipet. The top of the figure represents a sperm escaping using its thrust derived force. The sperm pulls free if its instantaneous thrust opposing the suction is greater than the suction force holding the sperm. The instantaneous thrust can be in any direction; thrust opposite the suction force is shown for clarity. The bottom of the figure shows the sperm escaping from the pipet using its torque-derived force. The sperm pries off the pipet; the lever arm is equal to $\ell$, and the torque acts around a fulcrum point on the edge of the pipet ($P$). In this illustration, the sperm exhibits a pitching motion; it could also show a rolling motion about its long axis so that it pivoted about a point near the side of its head, or a combination of the two motions. These motions correspond to the different components of torque on the head, as shown in Fig. 7*b*.

— 2. THEORETICAL CALCULATION OF THE MAGNITUDE AND ORIGIN OF THE PULLING FORCE OF A HUMAN SPERM ON A PIPET. The mechanical action by which a human sperm on a pipet exerts its maximum pulling force was not known, but there were only two major possibilities (Fig. 5). In the first, the sperm could pull directly away from the pipet, in which case the measured pulling force would equal the maximum forward or sideways thrust generated by the flagellum (thrust-derived force). Alternatively, the flagellum could act as a lever, producing a torque on the head and prying the head of the sperm off the pipet using the edge of the pipet as a fulcrum (torque-derived force). The torque-derived force was taken to be the calculated torque the flagellum can exert on the head divided by the distance from the center of the pipet to the outer edge of its rim, ~1.0 μm (range = 0.8–1.2 μm). The forces due to the thrust in the forward direction and the two perpendicular directions and also the force due to the torque on the head of the sperm were calculated for sperm on pipets as outlined in the Appendix. The maximum value of each force during a beat cycle was calculated.

The beat parameters measured and used in the calculation of the pulling forces of human sperm on pipets (see Methods) are shown in the top row of Table I. Our measurement of the ellipse described by the distal tip of the beating human sperm flagellum (mean half-axes of 1.3 and 6.4 μm) is in good agreement with that of Ishijima et al. (1986) (1.1 and 5.5 μm). The mean beat frequency of the human sperm captured on pipets for force measurement was 22/s. This corresponds to (by Eq. 3) the mean force of 20 μdyn measured. Since all the forces are proportional to frequency, they can simply be scaled to find the forces for other frequencies. The thrust and torque-derived forces were calculated using these parameters and the results are shown in Table I.

Thrusts calculated using the beat parameters measured for human sperm on pipets were in every case much smaller than the pulling forces measured with the pipets. Even if very large amplitudes (more than triple any observed) were used in the calculations, the thrusts were still nearly an order of magnitude smaller than the measured pulling forces. In contrast, the torque-derived force was always comparable with the measured pulling force. The measured force for a sperm with a beat frequency of 22 Hz was 20 μdyn, and the calculated torque-derived force for the same sperm was 19 μdyn. In contrast, the

TABLE I
FORCES EXERTED BY SPERM

| | Input Parameters | | | | | | Forces (microdynes) Calculated | | | Measured |
|---|---|---|---|---|---|---|---|---|---|---|
| | Flagellar length* | Flagellar radius‡ | Frequency | Beat shape ½ axes | Head dimensions* | Pipet radius | Torque | | Thrust | |
| | | | | | | | Pipet | Zona | | |
| | μm | μm | $s^{-1}$ | μm | μm | μm | | | | |
| Human (pipets) | 54 | 0.25 | 22 | 6.4, 1.3 | 2.2, 1.6 | 1.0 | 19 | (11) | 1.6 | 20 |
| Human (*zonae*) | 54 | 0.25 | 22 | 8.0, 1.2 | 2.2, 1.6 | — | (17) | 10 | 1.9 | — |
| Hamster (*zonae*) | 172 | 0.40 | 10 | 35, 5.4 | 7.6, 1.2 | — | (280) | 215 | 9.9 | — |
| Guinea pig (*zonae*) | 97 | 0.40 | 12 | 20, 3.0 | 5.0, 4.9 | — | (67) | 14 | 4.3 | — |
| Rabbit (*zonae*) | 50 | 0.40 | 25 | 10, 1.6 | 4.2, 2.4 | — | (24) | 9 | 2.8 | — |

The flagellar beat parameters observed for sperm on pipets and on *zonae*, measured as described in the text, are shown. These parameters were used to calculate (by the method given in the Appendix) the torque-derived and thrust-derived pulling forces.
The torque-derived forces in parentheses are shown for comparison. They represent the force that, for example, a sperm observed on the *zona* would have exerted on a pipet, or vice versa, given the same beat parameters. The force differs only because of the differing lever-arms for pipets and *zonae*.
The mean experimentally measured force and beat frequency for human sperm on pipets are shown.
*From Cummins and Woodall, 1985.
‡From Dresdner and Katz, 1981 (human and hamster); Friend et al., 1979 (guinea pig); and Stambaugh, 1978 (rabbit).

calculated thrust was only 1.6 μdyn. This led us to conclude that the maximum pulling force must have been torque- rather than thrust-derived, and hence that the sperm must pry itself off the pipet.

To confirm that the sperm does indeed pry itself off the pipet, video recordings of sperm coming off pipets were examined frame by frame. Fig. 6 shows a sperm coming off a pipet over the course of a single beat. In these photographs of single frames of the video recording, the sperm clearly pries its head off of the pipet using the rim of the pipet as a fulcrum.

Video recordings of a total of ten sperm coming off the pipets holding them were examined frame by frame. Of these ten, eight clearly pried off, one appeared to slide off, and one result was ambiguous.

— 3. THEORETICAL CALCULATION OF THE FORCE REQUIRED TO TETHER A SPERM ON THE *ZONA*. The force with which a sperm pulls on the *zona* can not be directly measured, but it can be calculated using the observed motions of the flagellum. The geometry of the sperm with respect to the pipet was chosen to mimic the geometry of the sperm on the *zona*. Therefore, it was assumed that the dominant pulling force of sperm on *zonae* is also torque-derived. The pulling force of sperm on the *zona* was calculated not only for human sperm, but also for hamster, guinea pig, and rabbit sperm. The beat parameters were measured for sperm on their homologous *zonae*. These beat parameters and the forces calculated using them are shown in Table I. The maximum thrust is also shown for comparison. The maximum instantaneous thrust was nearly perpendicular to the direction in which the sperm swims, but the net force is in the forward direction.

The lever-arm used to calculate the torque-derived pulling force of a sperm on a pipet, which was the distance from the pipet center to its outer edge, is not appropriate for sperm on *zonae*. The lever-arm on the *zona* is likely to be comparable with the distance from the center of the head to a point on the edge of the head (see Appendix). We calculated the maximum torque-derived force for each species about the edge of its head by the method given in the Appendix. The torque-derived force calculated with a 1.0-μm lever arm is also shown for comparison with human sperm on pipets.

It can be seen from Table I that for the four species examined, the maximum torque-derived force each sperm can exert on the *zona* exceeds by at least several-fold the maximum thrust that each can exert on the *zona*. Moreover, even the largest and most powerful of the sperm examined (hamster) can only exert a maximum pulling force of ~200 μdyn.

## II Strength of Bonds

The bonds between the sperm and the *zona* are affinity bonds, noncovalent bonds of the same type as antibody-antigen, receptor-ligand, and enzyme-substrate bonds, as first proposed by Lillie (1913). The tensile strength of affinity bonds can be inferred from their equilibrium binding behavior in solution: if both the free energy ($E$) of the bond and the effective length of the bond ($d$) are known, the tensile strength is, to a first approximation, simply $E/d$ (Zhurkov, 1965; Bell, 1978). Only a brief

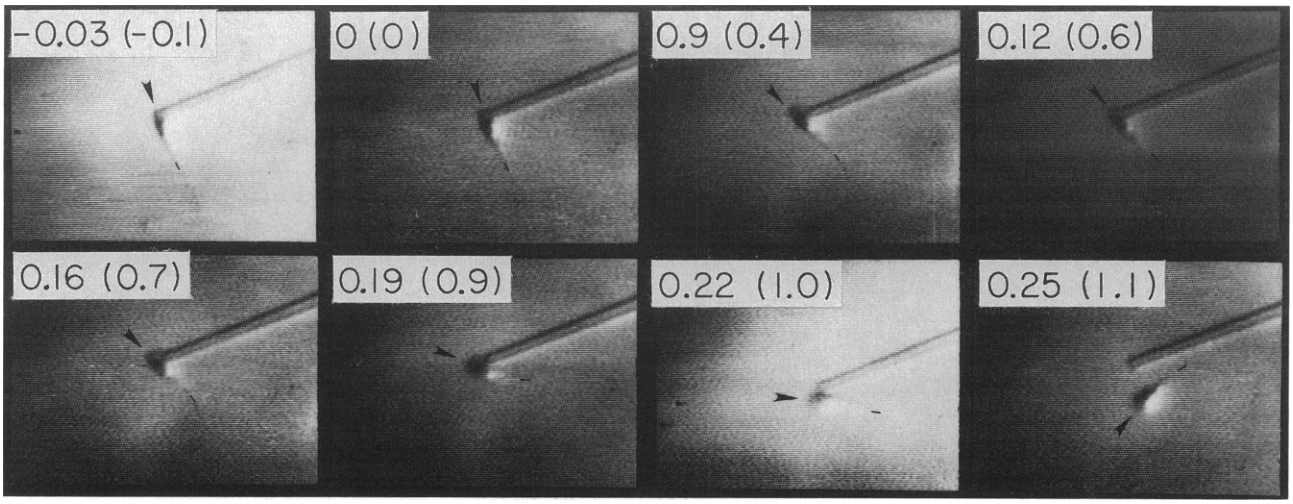


FIGURE 6 Details of a sperm prying off a pipet. In these single frames of a video recording, a sperm can clearly be seen to have pulled itself away with a prying action from the pipet which held it. This provides further evidence that sperm escaped from the pipets by means of their torque-derived force rather than their thrust. Fiduciary marks have been added: The arrows point back along the long axis of the head; the small line segments lie on the flagellum distal to the head. If the sperm had pulled directly off, rather than pried off, the orientation of the axis that these define would remain constant with respect of the pipet. The prying action of the escaping sperm is evidenced by the change in orientation of these marks. This particular sperm escaped the pipet by a combination of rolling and pitching motions. These frames cover 1.2 beat cycles (0.28 s). The sperm started to escape at $T = 0$. Each frame is labeled with the time and fraction of a beat cycle (*in parentheses*).

outline is given here. The free energy of affinity bonds is related to their binding constants ($K_b$) when free in solution by the equation

$$E = (kT)\ln(K_b/K_0). \quad (4)$$

$E$ is strictly the standard free energy ($\Delta G_0$) and $K_0$ is the binding constant of the standard state, 1 $M^{-1}$. Common values for the $K_b$ of biological affinity bonds range from $10^6$ to $10^{10}$ $M^{-1}$. The actual value of the binding constant is not critical here; because the term is logarithmic, the corresponding free energy from Eq. 4 is constant within 60% even with this four-order-of-magnitude range of binding constant.

The effective bond length is not well defined since pulling these bonds apart involves breaking many weaker bonds sequentially. However, the bond length lies between the lengths of the constituent weak bonds that contribute to the affinity bond (~1 Å), and the size of the entire binding site (~10 Å) (Pecht and Lancet, 1977).

The main uncertainty in the force calculation arises from the bond length, since the force is inversely proportional to it. The range of 1–10 Å leads to a corresponding 10-fold variation in the calculated force, while, as stated above, binding constants ranging over four orders of magnitude only produce a variation in the force of ~60%.

A more accurate calculation of the strength of an affinity bond requires accounting for the rates of diffusion to and from the binding sites, rotational diffusion to align the binding sites, and the activation energy that must be overcome to make or break the bond. Calculations of the strength of an affinity bond that account for these factors are treated elsewhere (Baltz, 1986; Baltz and Cone, in preparation), and some of these components have been accounted for in other treatments, e.g., Pecht and Lancet (1977). Taking these other factors into account, we calculate the maximum range possible for affinity bond strengths to be 6–250 μdyn with 40 μdyn being the most likely average value (Baltz, 1986; Baltz and Cone, in preparation). Again, the range accounts for the uncertainty primarily due to that in the bond length and size of the binding site and to a much lesser extent, to the range of possible binding constants.

The tensile strength of a covalent bond, in contrast to an affinity bond, is on the order of 500 μdyn (e.g., 400 for a C-C bond) (values of bond energy and length from Weast et al., 1986).

The tensile strength of an affinity bond as described above is that needed to quickly break the bond. However, a bond will eventually be broken by thermal energy in an average time that depends on its strength. Bell (1978), has developed a theoretical treatment of the strength of cell–cell adhesions that accounts for the finite lifetime of affinity bonds, which is directly applicable to the adhesion of sperm on the *zona* when the force producing tension on the adhesion is taken to be the pulling force of the sperm and only the molecules on the sperm are allowed to diffuse.

The value of the critical force at which the adhesion fails depends on the density of binding molecules on the *zona*, the density of complimentary molecules on the sperm, and the binding constant governing their interaction.

There are probably somewhat $<10^3$ accessible sites for sperm per square micron of *zona* surface (Green and Purves, 1984; Baltz, 1986), so the densities of the binding molecules on the *zona* and sperm was taken to be at most $10^3$ per square micron. By assuming the sperm-*zona* contact area to be ~1 square μm, the number of bonds found per square micron is the average number of sperm-*zona* bonds.

The above parameters were used with Bell's method for forces in the tens to hundreds of microdynes. The number of bonds needed to withstand these forces increased by only a fewfold ($<4\times$) when their finite lifetimes were accounted for in this way.

## DISCUSSION

### A How Many Bonds are Needed to Tether a Sperm?

The process by which the mammalian sperm penetrates the *zona* pellucida begins with the sperm head adhering to the *zona* surface. There has been considerable attention to the biology of this phenomenon, most of which has been from an ultrastructural or biochemical perspective. However, a detailed understanding of the mechanical and molecular basis of sperm-*zona* interaction will also require knowledge of how hard the sperm pulls on the *zona*, and how strong the specific sperm-*zona* bonds are. Thus, we determined and analyzed the forces which sperm on the *zona* can apply to their bound heads, i.e., those with which they can pull. We performed direct measurements and verified these by hydrodynamic calculations using measured parameters of the flagellar beat. The sperm pulling force was found to be under 30 μdyn for human sperm and only a few hundred microdynes even for the largest sperm (hamster) examined. The strength of the type of bond likely to exist between the sperm and the *zona* was calculated to be ~40 μdyn. This implies that a single bond is sufficient to tether many motile sperm, while the largest and most powerful sperm still require only a few. Even accounting for the finite lifetime of the bonds does not require that more than a very few bonds must exist to tether a sperm. This conclusion, that a single or few bonds are sufficient, is also valid for bond strengths within the calculated range of possible bond strengths (6–250 μdyn).

This result is consistent with the work of Green and Purves (1984) who determined by calculations that the thrust of a sperm could not significantly shorten the lifetimes of structural bonds within the *zona* material. Our more detailed calculations and direct measurements of the

sperm's pulling force showed a similar result for sperm-*zona* binding, even in light of the much greater torque-derived forces during this phase.

One implication of this result is that a very few bi- or multivalent binding molecules should be able to hold two motile sperm together. Agglutination of sperm should be possible when the number of antibodies is approximately the same as the number of sperm. Thus, our result is corroborated by the recent report by Isojima et al. (1987) of a monoclonal antibody against human sperm that can agglutinate sperm at concentrations that we have calculated (using their reported sperm and antibody concentrations) to be ~300 molecules of this antibody (reportedly an IgM) per sperm. Since the contact area between sperm can be <1 square micron, or ~1% of the surface area, this corresponds to fewer than 10 molecules tethering each sperm.

It appears then, that the vigorous motility of the flagellum, which is driven by many thousands of bonds between dynein and tubulin, is hardly sufficient to break even a single bond between a receptor and ligand, and cells live and move in a world in which their motion can be crucially altered by the formation or breaking of a single affinity bond.

### B Capacitation

Mammalian sperm must undergo a process called capacitation before they are able to fertilize the egg (Chang, 1951; Austin, 1951; Langlais and Roberts, 1985 for review) which for some species is accompanied by a marked increase in the vigor of motility termed hyperactivation (Yanigimachi, 1970; Yanigimachi and Usui, 1974; Mahi and Yanagimachi, 1976; Katz et al., 1978; Cummins, 1982; Suarez et al., 1983). Here, data for capacitated sperm on *zonae* were used in the theoretical calculations, but the human sperm used for pipet force measurements were not capacitated due primarily to the need for large populations of viable sperm. This approach is valid because capacitation does not greatly alter the mechanical behavior of human sperm, and thus the forces calculated with beat parameters of either group yielded forces that were nearly identical (Table I).

### C How Well do These Methods Mimic Sperm on *Zonae?*

In the calculations of the force exerted by a sperm on the *zona,* the sperm was assumed to lie flat with the major component of the flagellar beat parallel to the surface. How closely does this approach the actual situation on the *zona?*

In general, current belief is that the sperm of most mammals position their heads in a relatively flat orientation to the *zona* surface before the onset of penetration. This appears to be true both in vitro and in vivo, with or without the cumulus vestment present. Here, the sperm were seen to lie relatively flat on the *zona* in all four species: hamster, guinea pig, rabbit, and human and there are other reports of a similar orientation (human: Sundstrom, 1981; guinea pig: Yanigimachi, 1977; rabbit: Williams, 1972; hamster: Katz et al., 1986).

### D Implications for Sperm-*zona* Interaction

The physical details of the initial contact between the sperm and *zona* have been described in only a few species, e.g., guinea pig (Yanigimachi, 1977) and hamster (Katz et al., 1986; Drobnis et al., 1986). In these studies, most sperm were seen to first contact the cumulus-free *zona* by their tips, subsequently lie flat, and then penetrate.

The sperm is captured at the initial contact between the sperm tip and the *zona.* In this orientation, the pointed tip of the sperm can get little purchase adjacent to the point of attachment. Therefore, it would exert forwards and sideways thrust against the *zona* during tip-first adhesion of the sperm (Katz et al., 1986). Since the thrust is much smaller than the force needed to break a single affinity bond, the first bond made upon the tip-first meeting of the sperm and *zona* can result in the capture of the sperm.

If the egg and *zona* are surrounded by the cumulus, it may help restrain the sperm at the *zona* surface and allow tip-first penetration (Drobnis et al., 1986). However, cumulus-free eggs with intact zonae are fertilized in vitro with ease; mechanical constraint by the cumulus is not necessary for fertilization.

With nothing to restrain the sperm, the tip-first orientation is unstable (Katz et al., 1986). The motion of the motile sperm (pivoting about the point of attachment at the tip) will soon allow contact between the *zona* and the areas of the sperm head adjacent to the tip where more bonds will form further stabilizing the adhesion. This will continue until the maximum possible area of the sperm head is bound to the *zona,* and it is lying flat. Therefore, the observed transition from only the tip being bound, to the sperm head lying flat on the *zona,* results simply from the motion of the sperm and the adhesion between the sperm and *zona.*

Subsequently, as the sperm penetrates the *zona,* it can exert a shearing force on the *zona* that is less than its thrust (Green and Purves, 1984; Green, 1987), and it cannot break sperm-*zona* bonds or much perturb their lifetimes. The sperm head can progress forward through the *zona* only if all the bonds are eliminated. But, if the bonds were eliminated when the sperm was on the surface of the *zona,* the side-to-side motion of the head would allow it to follow the path of least resistance away from the *zona,* even a *zona* partially digested by acrosomal enzymes, and the sperm would escape.

How, then, can the sperm enter the *zona?* If the sperm lay flat against the *zona* surface, and if the bonds near the tip were eliminated first, the posterior portion of the head could remain bound while the anterior end is freed to probe

into the surface, as if it were hinged at the rear. The acrosome reaction could create this hinge, or another form of regulation could act to remove a subset of the sperm's *zona* receptors, or replace one set with another, before penetration.

A sperm lying flat on the *zona*, tethered, or hinged, only at the posterior of its head, will experience a large torque-derived force which moves its head from side to side, and a weaker, but constant, forward thrust. These motions will tend to create a shallow pit around the tip as the *zona* is dissolved by the acrosomal enzymes, and the forward thrust causes the tip to pivot about the tethered rear of the head into the layers of the *zona* material, trapping it. Indeed, in hamster, mouse, and rabbit, a smoothed area of the *zona* material is seen around the anterior of bound sperm in scanning electron micrographs, as if the sperm tip moved back and forth over it (Jedlicki and Barros, 1985), with tips of sperm in a more advanced state of penetration lodged under a flap of *zona* material (Jedlicki and Barros, 1985; Phillips, 1984; Williams, 1972). Thus, not only does the sperm lie flat because its motion and the adhesion makes this the most probable orientation, but this is also the most advantageous position from which bound sperm can begin to penetrate the *zona*.

Other mechanisms by which sperm enter the *zona* may exist, and the means used may vary among mammalian species. For example, the hamster sperm seems to be anchored onto the *zona* by an acrosomal shroud (Phillips, 1984; Talbot, 1985) which allows it to move into the *zona* but prevents escape, or the cumulus could be necessary in some species, although none have been reported. Without the addition of such mechanical aids, the mechanism we propose seems to be the simplest means by which the bound sperm can enter the *zona*.

Once the sperm tip has been inserted into the *zona* material, the sperm is constrained by the penetration slit. The adhesion at the posterior could then be eliminated to allow penetration.

Thus, the number and distribution of sperm-*zona* bonds must be carefully orchestrated to coincide with the binding and penetration sequence, so that the adhesion that captures the sperm at the initial sperm-*zona* contact and causes the head to lie flat, is followed by a looser attachment at the posterior as the tip is inserted, which is finally eliminated as penetration begins.

There is indeed evidence that sperm-*zona* bonds are regulated during binding and penetration. It has been shown in some species that the strength of sperm-*zona* adhesion changes during the course of sperm-*zona* interaction starting with a brief tight adhesion when the sperm first contact the *zona*, followed by a period of looser attachment, and finally another tight binding (Hartmann et al., 1972; Hartmann, 1983; Schmell and Gulyas, 1980; Bleil and Wassarman, 1983). One interpretation of these observations in light of our results is that the initial transitory tight binding is a burst of bond formation upon contact which persists until the sperm head is tacked down onto the *zona*, followed by a looser attachment when only the posterior hinge exists. The final tight binding could be the insertion of the tip into the *zona* or unregulated binding of unsuccessful sperm after the end of the regulated physiological binding.

Our results and analysis suggest that penetration of the *zona* pellucida by mammalian sperm must result from a highly organized and regulated sequence of events rather than being an inevitable result of the simple adhesion of a sperm with a beating flagellum to the *zona*. Sperm-*zona* bonds must capture the sperm, but cannot persist during penetration. Only if the bonds are eliminated in a regulated sequence will the action of the flagellum cause the sperm to enter, not escape from or remain stuck to, the *zona*.

## APPENDIX

## Resistive Force Calculations of Flagellar Thrust and Torque

Resistive force theory, as developed by Gray and Hancock (1955) and Lighthill (1975, 1976), was used to calculate the thrust and torque developed by a beating flagellum. The flagellum is considered to be a series of cylindrical segments, each interacting independently with the viscous environment. The force generated by each cylinder is the product of its velocity and its (tensorial) coefficient of resistance. Lighthill (1975, 1976) gives expressions for the coefficients of resistance per unit length of flagellum resolved tangential and normal to the flagellum:

$$K_t = \frac{2\pi\eta}{\ln(2q/a)} \tag{A1}$$

$$K_n = \frac{4\pi\eta}{\ln(2q/a) + 0.5}, \tag{A2}$$

where $q$ is 0.09 times the wavelength along the flagellum, $a$ is the radius of the flagellum, and $\eta$ is the viscosity of the medium.

The tangential and normal velocities of each segment are multiplied by their respective coefficients, yielding the normal and tangential forces. The total force is simply the vector sum of the forces on all the segments integrated along the flagellum. The torque about the head is obtained similarly, by taking the vector product of the force and the position vector at each point with the head as origin and then summing.

The waveform of the flagellum may be expressed as:

$$(x, y, z) = X(s - ct), Y(s - ct), Z(s - ct), \tag{A3}$$

where $x, y, z$ are the coordinates of any point on the flagellum, $s$ is distance along the flagellum, $c$ is the speed of wave propagation along the flagellum, and $t$ is time. The general expressions for the forces at each point on the flagellum as defined above are given in Lighthill (1975):

$$F_t = K_t(VX' - c) \tag{A4}$$

$$F_{nxt} = -K_n V(1 - X'^2)^{1/2}, \tag{A5}$$

where (see Fig. 7 *a*) $V$ is the speed of wave propagation along the flagellum in the head's frame of reference, with the distance taken in the $xyz$ coordinate system, and $X'$ is $dx/ds$.

There is no third force vector corresponding to force perpendicular to the $x$-$t$ plane since velocity components are confined to the $x$-$t$ plane.

Since the $n_{xt}$ and $t$ directions change depending on the position on the flagellum, it is necessary to find expressions for the forces in the $xyz$

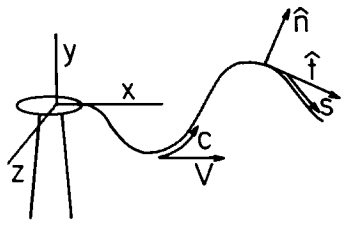


a

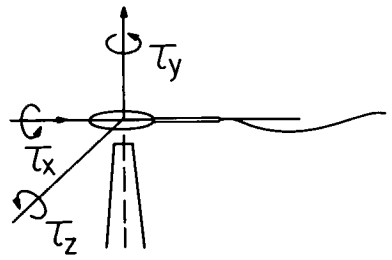


b

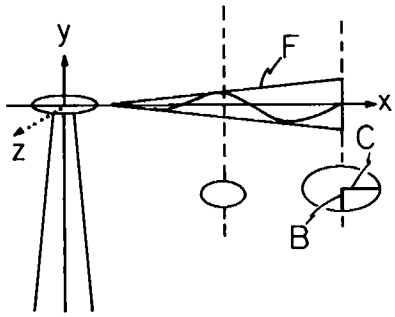


c

FIGURE 7 Coordinate systems and variables used in the calculation of forces exerted by a beating flagellum. (*a*) Coordinate system. The swimming sperm would proceed along the negative $x$ direction. The axis of the pipet, and minor axis of the beat cross-section lie along the $y$ axis. The major beat axis lies on the $z$ axis. The flagellar waveform propagates in the positive $x$ direction with a speed $V$ measured along the axis and a speed $c$ measured along the flagellum. $s$ is the arc-length along the flagellum at any point. **t** is the unit tangent vector and **n** is the unit normal vector in the $x$-$t$ plane. (*b*) Torques on the head of the sperm. Only the force due to $\tau_x$ and $\tau_z$ can pry the sperm off the pipet, producing rolling and pitching of the sperm respectively; the force due to $\tau_y$ would produce a yawing motion where the sperm merely rotates about the axis of the pipet, which would not help it to escape. (*c*) The waveform used for the calculations. The flagellar waveform ($F$) used was a conical helix with an elliptical cross-section. The largest cross-section, at the distal end of the flagellum, has a major half-axis $C$ in the $z$ direction and a minor half-axis $B$ in the $y$ direction.

coordinate system. Given the tangential unit vector, **t**:

$$\mathbf{t} = [X', Y', Z'] \tag{A6}$$

and the normal unit vector in the $xt$ plane:

$$\mathbf{n}_{xt} = [-(1 - X'^2)^{1/2}, X'Y'/(1 - X'^2)^{1/2}, X'Z'/(1 - X'^2)^{1/2}], \tag{A7}$$

the force vector, $[F_x, F_y, F_z]$, has components:

$$F_x = V\{K_t X'(X' - 1/\alpha) + K_n(1 - X'^2)\} \tag{A8}$$

$$F_y = VY'\{K_t(X' - 1/\alpha) - K_n X'\} \tag{A9}$$

$$F_z = VZ'(X' - 1/\alpha) - K_n X'\} \tag{A10}$$

where $\alpha = V/c$.

The torque is the vector product $rxF$, where **r** is the vector from the point (0, 0, 0) around which the torque is taken to the position $(x, y, z)$ on the flagellum. Thus, the torque ($\tau = [\tau_x, \tau_y, \tau_z]$) is:

$$\tau = [(F_z Y - F_y Z), (F_z X - F_x Z), (F_y X - F_x Y)]. \tag{A11}$$

This is the general expression. In our specific case only the components of torque which could act to pry the sperm off the pipet or zona are of interest. These are in the $xz$ plane (see Fig. 7 *b*), so only the $x$ and $z$ components of the torque need to be used:

$$\tau_{xz} = [\tau_x, 0, \tau_z] = [(F_z Y - F_y Z), 0, (F_y X - F_x Y)]. \tag{A12}$$

The components $\tau_x$ and $\tau_z$ are found by substituting the forces (Eqs. A8–A10) into this expression (A12). The total forces and torque are obtained by integrating these (A8–A10, A12) over the length of the flagellum.

The waveform that was used to approximate the beat of a flagellum was an elliptical helix in a conical envelope (Fig. 7 *c*). The equations describing it are:

$$X = \alpha s \tag{A13}$$

$$Y = (Bs/L) \cos 2(\pi/\lambda)(s - ct) \tag{A14}$$

$$Z = (Cs/L) \sin 2(\pi/\lambda)(s - ct). \tag{A15}$$

Here, $B$ and $C$ are amplitudes and $\lambda$ is the wavelength along the flagellum. Strictly speaking, $\alpha$ is not a constant but, as is discussed below, it can be approximated as such.

The forces were found using Eqs. A8–A10 with this waveform (Eqs. A13–A15) and integrating over the length of the flagellum:

$$F_x = [K_n - K_t](1 - \alpha^2)VL \tag{A16}$$

$$F_y = KVB \cos 2(\pi/\lambda)(L - ct) \tag{A17}$$

$$F_z = KVC \sin 2(\pi/\lambda)(L - ct), \tag{A18}$$

where $K = K_t(\alpha - 1/\alpha) - K_n\alpha$.

The torques were found similarly, using these forces to find the components of the torque $\tau_{xz} = [\tau_x, 0, \tau_z]$ (Eq. A12):

$$\tau_x = \frac{2\pi KVBCL}{3\lambda} \tag{A19}$$

$$\tau_z = \frac{KV \propto B}{L}\left\{L^2 \cos\frac{2\pi}{\lambda}(L - ct) - 2\left(\frac{\lambda}{2\pi}\right)^2 \cos\frac{2\pi}{\lambda}(L - ct)\right.$$

$$- \left(\frac{\lambda L}{\pi}\right) \sin \frac{2\pi}{\lambda}(L - ct) + 2\left(\frac{\lambda}{2\pi}\right)^2 \cos \frac{2\pi}{\lambda}(-ct)\Bigg\} - \frac{VK_nB}{L}\Bigg\{\left(\frac{\lambda}{2\pi}\right)^2 \cos \frac{2\pi}{\lambda}(L - ct) - \frac{\lambda L}{2\pi} \sin \frac{2\pi}{\lambda}(L - ct) + \left(\frac{\lambda}{2\pi}\right)^2 \cos 2\pi(-ct)\Bigg\}. \quad \text{(A20)}$$

Differentiation of Eqs. A16–A18 with respect to time yields the maximum values of the thrusts during a beat cycle:

$$F_x \max = [K_n - K_t](1 - \alpha^2)VL \quad \text{(A21)}$$

$$F_y \max = KVB \quad \text{(A22)}$$

$$F_z \max = KVC. \quad \text{(A23)}$$

Because $F_z$ max was always larger than either of the others, it was taken to be the maximum thrust during a beat.

The maximum values of the forces due to the torque on the head depend on both the value of the torque and the lever-arm chosen. For sperm on pipets, the lever arm was the outer radius of the pipet. Sperm on the *zona* are likely to pivot about the edge of their head when a torque is applied, since neither sperm nor *zona* exhibit appreciable compliance that would allow the sperm to peel off the *zona*: sperm are unusually rigid cells; in the suction apparatus, human sperm were not visibly deformed by a suction pressure two orders of magnitude greater than that which pulled 7 μm human red blood cells into the 1 μm opening of the pipet (data not shown) and the *zona* is also fairly rigid (Drobnis et al., 1985; Green, 1987). Thus, a sperm apparently must pry against the *zona* using the edge of its head as the fulcrum, as we assumed. Thus the lever arm was taken to be a radius of the head. The head of the sperm was assumed to be a prolate ellipsoid with major and minor axes as given in Table I. The torque-derived force at any time was then the magnitude of the torque divided by the radius of the head in the direction perpendicular to the torque vector. This radius was found according to:

$$r^2 = \frac{(\text{maj})^2 (\text{min})^2}{(\text{maj})^2 \sin^2(\theta) + (\text{min})^2 \cos^2(\theta)}, \quad \text{(A24)}$$

where (maj) and (min) are the major and minor axes, respectively, and $\theta$ is the angle describing the direction perpendicular to the torque vector.

In contrast to the maximum thrusts which were obtained by differentiating with respect to time, the maximum torque-derived force during each beat cycle was obtained numerically. The beat cycle was divided into 20 time segments. The torque-derived force obtained as the vector sum of $\tau_x$ and $\tau_z$ (Eqs. A19 and A20) divided by the radius (Eq. A24), was calculated at each of these times, and the greatest of these values was used as the maximum torque-derived force during a beat cycle.

Of the variables in the equations for force and torque, all are directly measured or simply calculated except for $\alpha$. $\alpha$ is $X'$, which represents the angle that the helix makes with the $x$ axis at any point. This is constant for a circular helix:

$$\alpha^2 = 1 - (P/\lambda)^2, \quad \text{(A25)}$$

where $P$ is the circumference of the circular cross section of the helix ($2\pi r$), but not strictly for an elliptical helix. However, without introducing much error, $\alpha$ can be approximated as a constant (as was done in the above derivations). We used:

$$\alpha^2 = 1 - (P'/\lambda)^2, \quad \text{(A26)}$$

where $P'$ is the approximate average circumference of the elliptical cross section (the exact circumference is given by an elliptical integral, but only differs significantly from this approximation if the helix is very flat). For the conical helix:

$$P' = \pi[(B^2 + C^2)/2]^{1/2}, \quad \text{(A27)}$$

where $B$ and $C$ are the half-axes of the largest cross section of the helix (at the distal end of the flagellum).

In the calculations of thrust- and torque-derived forces of sperm, the measured beat parameters shown in Table I were used in the above equations. The viscosity of the medium was taken to be 0.007 poise (the viscosity of the fluid surrounding a cumulus-free egg in vitro at 37°C). The velocity of propagation of the wave was calculated from the beat frequency and wavelength ($V = \alpha\lambda f$). Also, it was assumed that there was 1 wavelength on the flagellum; using 1.2 or 1.5 wavelengths on the flagellum (results not shown) had a relatively small effect on the calculated forces (smaller than 50% difference). All other variables were either measured directly, or taken from measurements in the literature, as cited.

We thank Dr. Richard A. Cardullo for his helpful discussions and critical reading of this manuscript, and Ms. Rachel Eugster for her careful proofreading.

This work was supported by National Institutes of Health grants HD16800 and HD12971.

*Received for publication 27 October 1987 and in final form 9 May 1988.*

## REFERENCES

Austin, C. R. 1951. Observations on the penetration of the sperm into the mammalian egg. *Aust. J. Sci. Res. B* 4:581–589.

Baltz, J. M. 1986. Measurement and calculation of the force necessary to hold a motile sperm; implications for the interactions between the sperm and the zona pellucida. Ph.D. thesis. The Johns Hopkins University, Baltimore, MD.

Bell, G. I. 1978. Models for the specific adhesion of cells to cells. *Science (Wash. DC)*. 200:618–627.

Bleil, J. D., and P. M. Wassarman. 1983. Sperm-egg interactions in the mouse: sequence of events and induction of the acrosome reaction by a zona pellucida glycoprotein. *Dev. Biol.* 95:317–324.

Bleil, J. D., and P. M. Wassarman, 1980. Mammalian sperm-egg interaction: identification of a glycoprotein in mouse egg zonae pellucidae possessing receptor activity for sperm. *Cell.* 20:873–882.

Bleil, J. D. and P. M. Wassarman. 1980(a). Structure and function of the zona pellucida: identification and characterization of the proteins of the mouse oocyte's zona pellucida. *Dev. Biol.* 76:185–202.

Cardullo, R. A. 1985. Oxygen metabolism, motility, and the maintenance of viability of caudal epididymal rat sperm. Ph.D. thesis. The Johns Hopkins University, Baltimore, MD.

Cardullo, R. A., and R. A. Cone. 1986. Mechanical immobilization of rat sperm does not change their oxygen consumption rate. *Biol. Reprod.* 34:820–830.

Chang, M. C. 1951. Fertiziling capacity of spermatozoa deposited into the fallopian tubes. *Nature (Lond.).* 168:697.

Cummins, J. M. 1982. Hyperactivated motility patterns of ram spermatozoa recovered from oviducts of mated ewes. *Gamete Res.* 6:53–64.

Cummins, J. M., and P. F. Woodall. 1985. On mammalian sperm dimensions. *J. Reprod. Fertil.* 75:153–175.

Denehy, M. A., D. Herbison-Evans, and B. V. Denehy. 1975. Rotational and oscillatory components of the tailwave in ram spermatozoa. *Biol. Reprod.* 13:289–297.

Dresdner, R. D., and D. F. Katz. 1981. Relationships of mammalian sperm motility and morphology to hydrodynamic aspects of cell function. *Biol. Reprod.* 25:920–930.

Dresdner, R. D., D. F. Katz, and S. A. Berger. 1980. The propulsion by large amplitude waves of uniflagellar micro-organisms of finite length. *J. Fluid Mech.* 97:591–621.

Drobnis, E. Z., J. M. Butterfield, and D. F. Katz. 1985. The mouse *zona pellucida* is more physically deformable in freshly ovulated eggs than in 2-cell embryos. *J. Cell Biol.* 101:377*a*. (Abstr.)

Drobnis, E. Z., A. I. Yudin, and D. F. Katz. 1986. Kinetic analysis of sperm penetrating the *zonae pellucidae* of cumulus-intact oocytes. *J. Cell Biol.* 103(2, Pt. 5): 241*a*. (Abstr.)

Friend, D. S., P. M. Elias, and I. Rudolf. 1979. Disassembly of the guinea pig sperm tail. *In* The spermatozoon. D. W. Fawcett and J. M. Bedford, editors. Urban & Schwartzberg, Inc., Baltimore, MD 157–172.

Gould, J. E., J. M. Overstreet, H. Yanagimachi, R. Yanagimachi, D. F. Katz, and F. W. Hanson. 1983. What functions of the sperm cell are measured by in vitro fertilization of *zona-free* hamster eggs? *Fertil. Steril.* 40(3):344–352.

Gray, J., and G. J. Hancock. 1955. The propulsion of sea-urchin spermatozoa. *J. Exp. Biol.* 32:802–814.

Green, D. P. L. 1987. Mammalian sperm cannot penetrate the *zona pellucida* solely by force. *Exp. Cell Res.* 169:31–38.

Green, D. P. L., and R. D. Purves. 1984. Mechanical hypothesis of sperm penetration. *Biophys. J.* 45:659–662.

Hartmann, J. F., R. B. Gwatkin, and C. F. Hutchison. 1972. Early contact interactions between mammalian gametes in vitro: evidence that the vitellus influences adherence between sperm and *zona pellucida*. *Proc. Natl. Acad. Sci. (USA).* 69(10):2767–2769.

Hartmann, J. F. 1983. Mammalian fertilization: gamete surface interactions in vitro. *In* Mechanism and control of animal fertilization. J. F. Hartmann, editor. Academic Press, Inc., N.Y. 325–364.

Ishijima, S., and H. Mohri. 1985. A quantitative description of flagellar movement in golden hamster spermatozoa. *J. Exp. Biol.* 114:463–475.

Ishijima, S., S. Oshio, and H. Mohri. 1986. Flagellar movement of human spermatozoa. *Gamete. Res.* 13:185–197.

Isojima, S., K. Kameda, Y. Tsuji, M. Shigeta, Y. Ikeda, and K. Koyama. 1987. Establishment and characterization of a human hybridoma secreting monoclonal antibody with high titers of sperm immobilizing and agglutinating activities against human sperm. *J. Reprod. Immunol.* 10:67–78.

Jedlicki, A., and C. Barros. 1985. Scanning electron microscope study of in vitro prepenetration gamete interactions. *Gamete Res.* 11:121–131.

Katz, D. F., G. N. Cherr, and H. Lambert. 1986. The evolution of hamster sperm motility during capacitation and interaction with the ovum vestments in vitro. *Gamete Res.* 14:333–346.

Katz, D. F., and N. J. deMestre. 1985. Thrust generation by mammalian spermatozoa against the *zona pellucida*. *Biophys. J.* 47(2, Pt. 2):123*a*. (Abstr.)

Katz, D. F., and R. Yanagimachi. 1981. Movement characteristics of hamster and guinea pig spermatozoa upon attachment to the *zona pellucida*. *Biol. Reprod.* 25:785–791.

Katz, D. F., R. Yanagimachi, and R. D. Dresdner. 1978. Movement characteristics and power output of guinea pig and hamster spermatozoa in relation to activation. *J. Reprod. Fertil.* 52:167–172.

Langlais, J., and K. D. Roberts. 1985. A molecular membrane model of sperm capacitation and the acrosome reaction of mammalian spermatozoa. *Gamete Res.* 12:183–224.

Lighthill, J. 1976. Flagellar hydrodynamics. *Siam (Soc. Ind. Appl. Math.).* 18:161–230.

Lighthill, J. 1975. Mathematical biofluiddynamics. Society for industrial and applied mathematics. Philadelphia, PA.

Lillie, F. R. 1913. The mechanism of fertilization. *Science (Wash. DC).* 38:524–528.

Lopez, L. C., E. M. Bayne, D. Litoff, N. L. Shaper, J. H. Shaper, and B. D. Shur. 1985. Receptor function of mouse sperm surface galactosyltransferase during fertilization. *J. Cell Biol.* 101:1501–1510.

Mahi, C. A., and R. Yangimachi. 1976. Maturation and sperm penetration of canine ovarian oocytes in vitro. *J. Exp. Zool.* 196:189–196.

O'Rand, M. G., J. E. Matthews, J. E. Welch, and S. J. Fisher. 1985. Identification of *zona* binding proteins of rabbit, pig, human, and mouse spermatozoa on nitrocellulose blots. *J. Exp. Zool.* 235:423–428.

Pecht, I., and D. Lancet. 1977. Kinetics of antibody-hapten interactions. *In* Chemical Relaxation in Molecular biology. I. Pecht and P. Rigler, editors. Springer-Verlag GmbH & Co. KG, Heidelberg, Berlin. 306–338.

Peterson, R. N., L. D. Russel, and W. P. Hunt. 1984. Evidence for specific binding of uncapacitated boar spermatozoa to porcine *zonae pellucidae* in vitro. *J. Exp. Zool.* 231:137–147.

Phillips, D. M. 1972. Comparative analysis of mammalian sperm motility. *J. Cell Biol.* 53:561–573.

Phillips, D. M. 1984. Problems in the analysis of mammalian fertilization. *In* Ultrastructure of reproduction. J. van Blerkom and P. M. Motta, editors. Martinus Nijhoff, Boston, MA. 166–175.

Rikmenspoel, R. 1965. The tail movement of bull spermatozoa. Observations and model calculations. *Biophys. J.* 5:365–392.

Schmell, E. D., and B. J. Gulyas. 1980. Mammalian sperm-egg recognition and binding in vitro. I. specificity of sperm interactions with live and fixed eggs in homologous and heterologous inseminations of hamster, mouse, and guinea pig oocytes. *Biol. Reprod.* 23:1075–1085.

Stambaugh, R. 1978. Enzymatic and morphological events in mammalian fertilization. *Gamete Res.* 1:65–85.

Suarez, S. S., D. F. Katz, and J. W. Overstreet. 1983. Movement characteristics and acrosomal status of rabbit spermatozoa recovered at the site and time of fertilization. *Biol. Reprod.* 29:1277–1287.

Sullivan, R., and G. Bleau. 1985. Interaction of isolated components from mammalian sperm and egg. *Gamete Res.* 12:101–116.

Sundstrom, P. 1981. Sperm penetration of the *zona pellucida* of human oocytes in vitro. *J. Ultrastruc. Res.* 76:328.

Talbot, P. 1985. Sperm penetration through oocytes investments in mammals. *Am. J. Anat.* 174:331–346.

Talbot, P., G. DiCarlantonio, P. Zao, J. Penkala, and L. T. Haimo. 1985. Motile cells which lack hyaluronidase can penetrate the hamster oocyte-cumulus complex. *Dev. Biol.* 108:387–398.

Wassarman, P. M. 1987. The biology and chemistry of fertilization. *Science (Wash. DC).* 235:553–560.

Weast, R. C., M. J. Astle, and W. H. Beyer. 1986. CRC Handbook of chemistry and physics. 67th ed. CRC Press, Inc. Boca Raton, FL.

Williams, W. L. 1972. Biochemistry of capacitation of spermatozoa. *In* Biology of Fertilization and Implantation. K. S. Moghissi and E. S. Hafez, editors. Charles C. Thomas, Springfield, IL. 19–53.

Yanagimachi, R. 1970. The movement of golden hamster spermatozoa before and after capacitation. *J. Repro. Fertil.* 23:193–196.

Yanagimachi, R. 1977. Specificity of sperm-egg interaction. *In* Immunobiology of Gametes. M. Edidin and K. Johnson, editors. Cambridge University Press, Cambridge, Great Britain.

Yanagimachi, R., and W. Usui. 1974. Calcium dependence of the acrosome reaction and activation of guinea pig spermatozoa. *Exp. Cell Res.* 89:161–174.

Zhurkov, S. N. 1965. Kinetic concept of the strength of solids. *Int. J. Frac. Mech.* 1:311–322.